

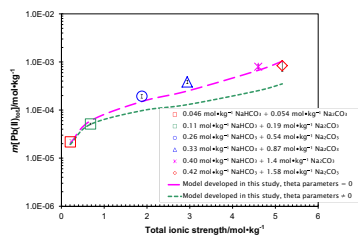
Experimental determination of lead carbonate solubility at high ionic strengths: a Pitzer model description

Yongliang Xiong¹

Received: 10 February 2015 / Accepted: 23 April 2015 / Published online: 6 May 2015
© Springer-Verlag Wien 2015

Abstract In this study, solubility measurements of lead carbonate, $\text{PbCO}_3(\text{cr})$, cerussite, as a function of total ionic strengths are conducted in the mixtures of NaCl and NaHCO_3 up to $I = 1.2 \text{ mol kg}^{-1}$ and in the mixtures of NaHCO_3 and Na_2CO_3 up to $I = 5.2 \text{ mol kg}^{-1}$, at room temperature ($22.5 \pm 0.5 \text{ }^\circ\text{C}$). The solubility constant ($\log K_s^\circ$) for cerussite was determined as -13.76 ± 0.15 (2σ) with a set of Pitzer parameters describing the specific interactions of $\text{PbCO}_3(\text{aq})$, $\text{Pb}(\text{CO}_3)_2^{2-}$, and $\text{Pb}(\text{CO}_3)\text{Cl}^-$ with the bulk-supporting electrolytes, based on the Pitzer model. The model developed in this work can reproduce the experimental results including model-independent solubility values from the literature over a wide range of ionic strengths with satisfactory accuracy. The model is expected to find applications in numerous fields, including the accurate description of chemical behavior of lead in geological repositories, the modeling of formation of oxidized Pb–Zn ore deposits, and the environmental remediation of lead contamination.

Graphical abstract



✉ Yongliang Xiong
yxiong@sandia.gov

¹ Sandia National Laboratories (SNL), Carlsbad Programs Group, 4100 National Parks Highway, Carlsbad, NM 88220, USA

Keywords Lead contamination remediation · Cerussite · Oxidized lead–zinc ore deposits · Solution chemistry · Nuclear waste management · Waste Isolation Pilot Plant

Introduction

Lead carbonate, $\text{PbCO}_3(\text{cr})$, with the mineral name cerussite, is important to many fields. In the following, a few examples are provided to illustrate its importance. In the field of environmental remediation of lead contamination, it has been found that Pb^{2+} can be immobilized from aqueous solutions using calcite or aragonite, owing to the fact that Pb^{2+} can be precipitated as cerussite on the surface of the CaCO_3 [1]. As demonstrated by Gamsjäger et al. [1], the concentration of Pb^{2+} in solutions under certain conditions can be reduced below environmentally tolerated concentrations after precipitation of cerussite. A recent study also suggests that while lead oxalate, $\text{PbC}_2\text{O}_4(\text{cr})$, should be the solubility-determining phase for lead in the soil solutions from acidic to near neutral pH, cerussite is the solubility-determining phase for lead in alkaline pHs [2]. In the field of mineral deposits, cerussite is the dominant ore mineral in non-sulfide, oxidized lead–zinc ore deposits in the world, e.g., [3]. Cerussite in those non-sulfide lead–zinc ore deposits was formed when lead and zinc sulfides in the primary lead–zinc sulfide deposits were oxidized; Pb^{2+} and Zn^{2+} were transported into the subsurface environments, and Pb^{2+} and Zn^{2+} were precipitated as their respective carbonates.

In the field of nuclear waste management, cerussite is expected to play a significant role. The Waste Isolation Pilot Plant (WIPP) is a U.S. Department of Energy (DOE) repository in southeast New Mexico for defense-related transuranic (TRU) waste. The repository, which opened in

March 1999, is located at a subsurface depth of 655 m in the Salado formation, a Permian bedded-salt formation. In the waste stream, lead is already present and it is also planned to use a significant amount of lead as a radiation-shielding material for wastes with significant γ -radiation placed in the WIPP. Carbonate is an important inorganic ligand in the WIPP brines such as generic weep brine (GWB) from the Salado formation at the stratigraphic horizon of the repository, and Energy Research and Development Administration (WIPP well) 6 (ERDA-6) brine from the underlying Castile formation [4]. When lead is corroded under anoxic conditions in carbonate-containing brines, cerussite is expected to form.

In addition, cerussite is also proposed as a waste form for geological disposal of radioactive ^{14}C generated in the heavy-water moderator systems of nuclear reactors [5]. Therefore, the accurate knowledge of solubilities of cerussite in a wide range of ionic strengths has important bearings on the chemical behavior of both cerussite formed under repository conditions, and cerussite as a waste form for radioactive ^{14}C introduced into a geological repository.

In this work, a long-term study on the solubilities of cerussite in $\text{NaHCO}_3 + \text{NaCl}$, and $\text{NaHCO}_3 + \text{Na}_2\text{CO}_3$ solutions at room temperature and at high ionic strengths up to 5.16 mol kg^{-1} conducted at Sandia National Laboratories (SNL) Carlsbad Facility is presented. In conjunction with the thermodynamic parameters from the literature, a Pitzer model is developed for the accurate descriptions of the $\text{Na}^+ - \text{Pb}^{2+} - \text{Cl}^- - \text{HCO}_3^- - \text{CO}_3^{2-}$ system.

Results and discussion

The results for the experiments in $\text{NaCl} + \text{NaHCO}_3$ and $\text{NaHCO}_3 + \text{Na}_2\text{CO}_3$ solutions are presented in Tables 1 and 2, respectively. Figure 1 displays dissolved total lead concentrations as a function of experimental time. From Fig. 1, we can see that the steady-state dissolved total lead concentrations were attained for all experiments after 900 days. Therefore, the experimental data after 900 days in $\text{NaCl} + \text{NaHCO}_3$ solutions are considered as the equilibrium values, and are used in the following modeling. Notice that the experimental data are quite consistent for the experiments with NaHCO_3 concentrations higher than $0.0086 \text{ mol kg}^{-1}$, such as the experiments with 0.43 and 0.86 mol kg^{-1} NaHCO_3 . However, there is a scatter in the experimental data for the experiment with the lowest concentration of NaHCO_3 , i.e., $0.0086 \text{ mol kg}^{-1}$ NaHCO_3 . Figure 2 illustrates dissolved total lead concentrations as a function of experimental time in the mixtures of $\text{NaHCO}_3 + \text{Na}_2\text{CO}_3$. It is clear from Fig. 2 that the steady-state concentrations were attained after 200 days for all of the experiments. Consequently, the experimental data after

200 days in the mixtures of $\text{NaHCO}_3 + \text{Na}_2\text{CO}_3$ are considered as the equilibrium values, and are used in the following modeling. It is assumed that steady-state concentrations represent equilibrium concentrations, as the duration of experiments in this work, up to 1461 days, is significantly longer than previous studies such as those of Nasanen et al. [6], and Bilinski and Schindler [7] under similar conditions. For instance, the experiments of Nasanen et al. [6] lasted only for up to 52 h (i.e., 2.2 days).

In Fig. 3, solubilities of cerussite represented by dissolved total lead concentrations as a function of total ionic strengths in the mixtures of 0.15 or 0.30 mol kg^{-1} NaCl and varying concentrations of NaHCO_3 are shown. Figure 3 indicates that solubilities have a strong dependence on ionic strength, indicating the increase in solubility with total ionic strength. At the lowest total ionic strength (i.e., $\sim 0.2 \text{ mol kg}^{-1}$), the solubility is in the order of $10^{-6} \text{ mol kg}^{-1}$. In contrast, at the highest total ionic strength (i.e., $\sim 1.2 \text{ mol kg}^{-1}$), the solubility of cerussite is in the order of $10^{-4} \text{ mol kg}^{-1}$, indicating an increase in two orders of magnitude.

Similarly, solubilities of cerussite as a function of total ionic strengths in the mixtures of NaHCO_3 and Na_2CO_3 are displayed in Fig. 4. Again, Fig. 4 suggests that solubilities of cerussite have a strong dependence on total ionic strength with rising solubilities with increasing ionic strength. For instance, the solubility is in the order of $10^{-5} \text{ mol kg}^{-1}$ at $I = \sim 0.2 \text{ mol kg}^{-1}$ (Fig. 4; Table 2), increasing to an order of $10^{-3} \text{ mol kg}^{-1}$ at $I = \sim 5.2 \text{ mol kg}^{-1}$.

In the following, the $\text{Na}^+ - \text{Pb}^{2+} - \text{Cl}^- - \text{HCO}_3^- - \text{CO}_3^{2-}$ system is thermodynamically modeled based on solubility data of cerussite described above. Under the experimental conditions in this work, the contributions from the lead hydroxyl complexes to the solubility are insignificant and negligible. Therefore, the lead hydroxyl complexes are not considered in the modeling. The lead hydroxyl complexes will be modeled in a future, separate publication based on the experimental solubility data in alkaline and hyperalkaline solutions.

The dissolution reaction for $\text{PbCO}_3(\text{cr})$ can be expressed as



The corresponding solubility product constant of $\text{PbCO}_3(\text{cr})$ at infinite dilution can be cast as follows:

$$K_s^o = \frac{a_{\text{Pb}^{2+}} \times a_{\text{CO}_3^{2-}}}{a_{\text{PbCO}_3(\text{cr})}} \quad (2)$$

In the modeling, the aqueous lead species included are Pb^{2+} , PbCl^+ , $\text{PbCl}_2(\text{aq})$, PbCl_3^- , $\text{PbCO}_3(\text{aq})$, $\text{Pb}(\text{CO}_3)_2^{2-}$, and $\text{Pb}(\text{CO}_3)\text{Cl}^-$. In the work of Xiong et al. [2], the thermodynamic parameters for description of Pb^{2+} , PbCl^+ , $\text{PbCl}_2(\text{aq})$, PbCl_3^- have been presented.

Table 1 Experimental results concerning solubility of $\text{PbCO}_3(\text{cr})$ in NaHCO_3 solutions with 0.15–0.3 mol kg^{-1} NaCl produced in this work at 22.5 ± 0.5 °C

Experimental number	Day	$\Sigma\text{Pb}/\text{mol kg}^{-1}$	$\Sigma\text{Na}/\text{mol kg}^{-1}$	$\Sigma\text{Cl}/\text{mol kg}^{-1}$	pmH ^a	$\Sigma\text{CO}_3/\text{mol kg}^{-1}$
PbCO ₃ -0.01/0.15-1	741	1.12E-06	0.1586	0.15	9.10	8.60E-03
PbCO ₃ -0.01/0.15-2	741	7.10E-07	0.1586	0.15	9.37	8.60E-03
PbCO ₃ -0.05/0.15-1	741	2.94E-06	0.193	0.15	9.04	4.30E-02
PbCO ₃ -0.05/0.15-2	741	2.94E-06	0.193	0.15	9.03	4.30E-02
PbCO ₃ -0.5/0.15-1	741	2.58E-05	0.58	0.15	8.82	4.30E-01
PbCO ₃ -0.5/0.15-2	741	2.69E-05	0.58	0.15	8.92	4.30E-01
PbCO ₃ -1.0/0.15-1	741	5.83E-05	1.01	0.15	8.77	8.60E-01
PbCO ₃ -1.0/0.15-2	741	6.04E-05	1.01	0.15	8.70	8.60E-01
PbCO ₃ -1.0/0.30-1	741	6.68E-05	1.16	0.3	8.72	8.60E-01
PbCO ₃ -1.0/0.30-2	741	7.13E-05	1.16	0.3	8.70	8.60E-01
PbCO ₃ -0.01/0.15-1	1020	5.83E-07	0.1586	0.15	8.71	8.60E-03
PbCO ₃ -0.01/0.15-2	1020	3.92E-06	0.1586	0.15	9.17	8.60E-03
PbCO ₃ -0.05/0.15-1	1020	4.96E-06	0.193	0.15	8.94	4.30E-02
PbCO ₃ -0.05/0.15-2	1020	4.73E-06	0.193	0.15	9.09	4.30E-02
PbCO ₃ -0.5/0.15-1	1020	9.64E-05	0.58	0.15	9.68	4.30E-01
PbCO ₃ -0.5/0.15-2	1020	4.48E-05	0.58	0.15	9.08	4.30E-01
PbCO ₃ -1.0/0.15-1	1020	8.90E-05	1.01	0.15	8.96	8.60E-01
PbCO ₃ -1.0/0.15-2	1020	8.11E-05	1.01	0.15	8.87	8.60E-01
PbCO ₃ -1.0/0.30-1	1020	1.25E-04	1.16	0.3	9.06	8.60E-01
PbCO ₃ -1.0/0.30-2	1020	9.16E-05	1.16	0.3	8.90	8.60E-01
PbCO ₃ -0.01/0.15-1	1069	1.59E-06	0.1586	0.15	8.68	8.60E-03
PbCO ₃ -0.01/0.15-2	1069	2.23E-06	0.1586	0.15	9.15	8.60E-03
PbCO ₃ -0.05/0.15-1	1069	5.14E-06	0.193	0.15	8.98	4.30E-02
PbCO ₃ -0.05/0.15-2	1069	5.03E-06	0.193	0.15	9.10	4.30E-02
PbCO ₃ -0.5/0.15-1	1069	7.14E-05	0.58	0.15	9.55	4.30E-01
PbCO ₃ -0.5/0.15-2	1069	4.65E-05	0.58	0.15	9.09	4.30E-01
PbCO ₃ -1.0/0.15-1	1069	9.94E-05	1.01	0.15	8.96	8.60E-01
PbCO ₃ -1.0/0.15-2	1069	9.28E-05	1.01	0.15	8.89	8.60E-01
PbCO ₃ -1.0/0.30-1	1069	1.27E-04	1.16	0.3	9.07	8.60E-01
PbCO ₃ -1.0/0.30-2	1069	1.06E-04	1.16	0.3	8.90	8.60E-01
PbCO ₃ -0.01/0.15-1	1118	5.96E-07	0.1586	0.15	8.57	8.60E-03
PbCO ₃ -0.01/0.15-2	1118	1.31E-06	0.1586	0.15	9.24	8.60E-03
PbCO ₃ -0.05/0.15-1	1118	3.69E-06	0.193	0.15	9.09	4.30E-02
PbCO ₃ -0.05/0.15-2	1118	4.35E-06	0.193	0.15	9.19	4.30E-02
PbCO ₃ -0.5/0.15-1	1118	6.57E-05	0.58	0.15	9.59	4.30E-01
PbCO ₃ -0.5/0.15-2	1118	5.04E-05	0.58	0.15	9.16	4.30E-01
PbCO ₃ -1.0/0.15-1	1118	1.05E-04	1.01	0.15	9.04	8.60E-01
PbCO ₃ -1.0/0.15-2	1118	9.72E-05	1.01	0.15	8.98	8.60E-01
PbCO ₃ -1.0/0.30-1	1118	1.38E-04	1.16	0.3	9.15	8.60E-01
PbCO ₃ -1.0/0.30-2	1118	1.08E-04	1.16	0.3	8.99	8.60E-01
PbCO ₃ -0.01/0.15-1	1167	3.49E-06	0.1586	0.15	8.60	8.60E-03
PbCO ₃ -0.01/0.15-2	1167	1.42E-06	0.1586	0.15	9.14	8.60E-03
PbCO ₃ -0.05/0.15-1	1167	4.02E-06	0.193	0.15	9.01	4.30E-02
PbCO ₃ -0.05/0.15-2	1167	4.44E-06	0.193	0.15	9.11	4.30E-02
PbCO ₃ -0.5/0.15-1	1167	6.24E-05	0.58	0.15	9.49	4.30E-01
PbCO ₃ -0.5/0.15-2	1167	5.04E-05	0.58	0.15	9.09	4.30E-01
PbCO ₃ -1.0/0.15-1	1167	1.09E-04	1.01	0.15	8.97	8.60E-01
PbCO ₃ -1.0/0.15-2	1167	9.89E-05	1.01	0.15	8.92	8.60E-01

Table 1 continued

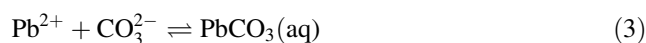
Experimental number	Day	$\Sigma\text{Pb/mol kg}^{-1}$	$\Sigma\text{Na/mol kg}^{-1}$	$\Sigma\text{Cl/mol kg}^{-1}$	pmH ^a	$\Sigma\text{CO}_3/\text{mol kg}^{-1}$
PbCO ₃ -1.0/0.30-1	1167	1.13E-04	1.16	0.3	9.08	8.60E-01
PbCO ₃ -1.0/0.30-2	1167	1.43E-04	1.16	0.3	8.93	8.60E-01
PbCO ₃ -0.01/0.15-1	1293	1.11E-06	0.1586	0.15	8.52	8.60E-03
PbCO ₃ -0.01/0.15-2	1293	2.16E-06	0.1586	0.15	9.22	8.60E-03
PbCO ₃ -0.05/0.15-1	1293	6.25E-06	0.193	0.15	9.07	4.30E-02
PbCO ₃ -0.05/0.15-2	1293	6.73E-06	0.193	0.15	9.17	4.30E-02
PbCO ₃ -0.5/0.15-1	1293	7.49E-05	0.58	0.15	9.54	4.30E-01
PbCO ₃ -0.5/0.15-2	1293	5.27E-05	0.58	0.15	9.17	4.30E-01
PbCO ₃ -1.0/0.15-1	1293	1.13E-04	1.01	0.15	9.06	8.60E-01
PbCO ₃ -1.0/0.15-2	1293	9.78E-05	1.01	0.15	9.01	8.60E-01
PbCO ₃ -1.0/0.30-1	1293	1.37E-04	1.16	0.3	9.16	8.60E-01
PbCO ₃ -1.0/0.30-2	1293	1.30E-04	1.16	0.3	9.03	8.60E-01
PbCO ₃ -0.01/0.15-1	1379	1.97E-07	0.1586	0.15	8.50	8.60E-03
PbCO ₃ -0.01/0.15-2	1379	1.87E-06	0.1586	0.15	9.16	8.60E-03
PbCO ₃ -0.05/0.15-1	1379	3.73E-06	0.193	0.15	9.05	4.30E-02
PbCO ₃ -0.05/0.15-2	1379	4.27E-06	0.193	0.15	9.14	4.30E-02
PbCO ₃ -0.5/0.15-1	1379	6.55E-05	0.58	0.15	9.50	4.30E-01
PbCO ₃ -0.5/0.15-2	1379	6.69E-05	0.58	0.15	9.10	4.30E-01
PbCO ₃ -1.0/0.15-1	1379	1.22E-04	1.01	0.15	8.99	8.60E-01
PbCO ₃ -1.0/0.15-2	1379	1.19E-04	1.01	0.15	8.96	8.60E-01
PbCO ₃ -1.0/0.30-1	1379	1.61E-04	1.16	0.3	9.09	8.60E-01
PbCO ₃ -1.0/0.30-2	1379	1.20E-04	1.16	0.3	8.97	8.60E-01
PbCO ₃ -0.01/0.15-1	1461	8.95E-07	0.1586	0.15	8.52	8.60E-03
PbCO ₃ -0.01/0.15-2	1461	1.04E-05	0.1586	0.15	9.15	8.60E-03
PbCO ₃ -0.05/0.15-1	1461	3.65E-06	0.193	0.15	9.04	4.30E-02
PbCO ₃ -0.05/0.15-2	1461	1.44E-05	0.193	0.15	9.12	4.30E-02
PbCO ₃ -0.5/0.15-1	1461	8.17E-05	0.58	0.15	9.14	4.30E-01
PbCO ₃ -0.5/0.15-2	1461	6.25E-05	0.58	0.15	9.12	4.30E-01
PbCO ₃ -1.0/0.15-1	1461	1.53E-04	1.01	0.15	9.01	8.60E-01
PbCO ₃ -1.0/0.15-2	1461	1.02E-04	1.01	0.15	8.98	8.60E-01
PbCO ₃ -1.0/0.30-1	1461	1.32E-04	1.16	0.3	9.11	8.60E-01
PbCO ₃ -1.0/0.30-2	1461	1.43E-04	1.16	0.3	8.98	8.60E-01

^a pH readings obtained using a pH electrode were first converted to hydrogen ion concentrations on molar scale (pcH) by applying correction factors compiled [16], and then converted to hydrogen ion concentrations on molal scale (pmH) using the equation of Xiong et al. [17]

The lead carbonate species, PbCO₃(aq), Pb(CO₃)₂²⁻, and mixed complex, Pb(CO₃)Cl⁻ are recommended by Powell et al. [8] and Woosley and Millero [9]. In addition, Powell et al. [8] mentioned the complex PbHCO₃⁻. However, the strength of this complex is very weak in comparison with PbCO₃(aq), Pb(CO₃)₂²⁻, and PbCO₃Cl⁻. Therefore, it is not included in the model developed in this analysis.

Chloride ion (Cl⁻) forms a relatively strong ternary complex with CO₃²⁻ and Pb²⁺ [9], i.e., Pb(CO₃)Cl⁻, in comparison with the binary lead chloride complexes. For, instance, the log β₁₁ for Pb(CO₃)Cl⁻ and log β₁ for PbCl⁺ are 7.23 [9] and 1.48 [10], respectively. Therefore, Pb(CO₃)Cl⁻ is considered as well as PbCO₃(aq) and Pb(CO₃)₂²⁻ in the modeling.

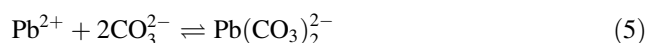
The formation reaction for PbCO₃(aq) is written as



The corresponding cumulative formation constant at infinite dilution is

$$\beta_1^0 = \frac{a_{\text{PbCO}_3(\text{aq})}}{a_{\text{Pb}^{2+}} \times a_{\text{CO}_3^{2-}}} \quad (4)$$

Similarly, the cumulative formation reaction for Pb(CO₃)₂²⁻ can be written as



The corresponding cumulative formation constant at infinite dilution should be

Table 2 Experimental results concerning solubility of $\text{PbCO}_3(\text{cr})$ in the mixtures of NaHCO_3 and Na_2CO_3 produced in this work at 22.5 ± 0.5 °C

Experimental number	Day	$\Sigma\text{Pb}/\text{mol kg}^{-1}$	$\Sigma\text{Na}/\text{mol kg}^{-1}$	pmH ^a	$\Sigma\text{CO}_3/\text{mol kg}^{-1}$
PbCO ₃ -buffer A-1	238	2.21E-05	0.154	9.86	0.100
PbCO ₃ -buffer A-2	238	2.19E-05	0.154	9.83	0.100
PbCO ₃ -buffer B-1	238	5.03E-05	0.49	9.79	0.300
PbCO ₃ -buffer B-2	238	5.20E-05	0.49	9.78	0.300
PbCO ₃ -buffer C-1	238	1.95E-04	1.34	10.04	0.800
PbCO ₃ -buffer C-2	238	1.92E-04	1.34	10.04	0.800
PbCO ₃ -buffer D-1	238	3.80E-04	2.07	10.28	1.200
PbCO ₃ -buffer D-2	238	3.97E-04	2.07	10.29	1.200
PbCO ₃ -buffer E-1	238	9.01E-04	3.2	10.65	1.800
PbCO ₃ -buffer E-2	238	7.88E-04	3.2	10.65	1.800
PbCO ₃ -buffer F-1	238	6.97E-04	3.58	10.76	2.000
PbCO ₃ -buffer F-2	238	5.88E-04	3.58	10.79	2.000
PbCO ₃ -buffer A-1	287	2.33E-05	0.154	9.86	0.100
PbCO ₃ -buffer A-2	287	2.23E-05	0.154	9.86	0.100
PbCO ₃ -buffer B-1	287	5.05E-05	0.49	9.84	0.300
PbCO ₃ -buffer B-2	287	5.19E-05	0.49	9.85	0.300
PbCO ₃ -buffer C-1	287	1.95E-04	1.34	10.10	0.800
PbCO ₃ -buffer C-2	287	1.97E-04	1.34	10.11	0.800
PbCO ₃ -buffer D-1	287	3.82E-04	2.07	10.35	1.200
PbCO ₃ -buffer D-2	287	3.88E-04	2.07	10.37	1.200
PbCO ₃ -buffer E-1	287	7.94E-04	3.2	10.73	1.800
PbCO ₃ -buffer E-2	287	7.94E-04	3.2	10.73	1.800
PbCO ₃ -buffer F-1	287	8.33E-04	3.58	10.85	2.000
PbCO ₃ -buffer F-2	287	8.07E-04	3.58	10.85	2.000
PbCO ₃ -buffer A-1	336	2.40E-05	0.154	9.85	0.100
PbCO ₃ -buffer A-2	336	2.31E-05	0.154	9.83	0.100
PbCO ₃ -buffer B-1	336	5.20E-05	0.49	9.82	0.300
PbCO ₃ -buffer B-2	336	5.25E-05	0.49	9.82	0.300
PbCO ₃ -buffer C-1	336	2.06E-04	1.34	10.05	0.800
PbCO ₃ -buffer C-2	336	2.08E-04	1.34	10.06	0.800
PbCO ₃ -buffer D-1	336	3.95E-04	2.07	10.27	1.200
PbCO ₃ -buffer D-2	336	4.07E-04	2.07	10.29	1.200
PbCO ₃ -buffer E-1	336	8.04E-04	3.2	10.64	1.800
PbCO ₃ -buffer E-2	336	7.91E-04	3.2	10.65	1.800
PbCO ₃ -buffer F-1	336	8.76E-04	3.58	10.75	2.000
PbCO ₃ -buffer F-2	336	8.53E-04	3.58	10.76	2.000
PbCO ₃ -buffer A-1	385	2.24E-05	0.154	9.84	0.100
PbCO ₃ -buffer A-2	385	2.20E-05	0.154	9.84	0.100
PbCO ₃ -buffer B-1	385	5.24E-05	0.49	9.84	0.300
PbCO ₃ -buffer B-2	385	5.15E-05	0.49	9.83	0.300
PbCO ₃ -buffer C-1	385	2.05E-04	1.34	10.07	0.800
PbCO ₃ -buffer C-2	385	2.01E-04	1.34	10.07	0.800
PbCO ₃ -buffer D-1	385	4.05E-04	2.07	10.30	1.200
PbCO ₃ -buffer D-2	385	4.08E-04	2.07	10.31	1.200
PbCO ₃ -buffer E-1	385	8.20E-04	3.2	10.66	1.800
PbCO ₃ -buffer E-2	385	8.46E-04	3.2	10.67	1.800
PbCO ₃ -buffer F-1	385	8.46E-04	3.58	10.78	2.000
PbCO ₃ -buffer F-2	385	9.73E-04	3.58	10.80	2.000

Table 2 continued

Experimental number	Day	$\Sigma\text{Pb/mol kg}^{-1}$	$\Sigma\text{Na/mol kg}^{-1}$	pmH ^a	$\Sigma\text{CO}_3/\text{mol kg}^{-1}$
PbCO ₃ -buffer A-1	511	2.09E-05	0.154	9.84	0.100
PbCO ₃ -buffer A-2	511	2.09E-05	0.154	9.84	0.100
PbCO ₃ -buffer B-1	511	5.14E-05	0.49	9.85	0.300
PbCO ₃ -buffer B-2	511	5.06E-05	0.49	9.85	0.300
PbCO ₃ -buffer C-1	511	1.81E-04	1.34	10.09	0.800
PbCO ₃ -buffer C-2	511	1.80E-04	1.34	10.09	0.800
PbCO ₃ -buffer D-1	511	3.65E-04	2.07	10.33	1.200
PbCO ₃ -buffer D-2	511	3.68E-04	2.07	10.34	1.200
PbCO ₃ -buffer E-1	511	7.56E-04	3.2	10.70	1.800
PbCO ₃ -buffer E-2	511	7.48E-04	3.2	10.69	1.800
PbCO ₃ -buffer F-1	511	8.54E-04	3.58	10.81	2.000
PbCO ₃ -buffer F-2	511	8.07E-04	3.58	10.82	2.000
PbCO ₃ -buffer A-1	601	2.17E-05	0.154	9.83	0.100
PbCO ₃ -buffer A-2	601	2.20E-05	0.154	9.83	0.100
PbCO ₃ -buffer B-1	601	5.36E-05	0.49	9.84	0.300
PbCO ₃ -buffer B-2	601	5.21E-05	0.49	9.83	0.300
PbCO ₃ -buffer C-1	601	1.97E-04	1.34	10.07	0.800
PbCO ₃ -buffer C-2	601	1.96E-04	1.34	10.07	0.800
PbCO ₃ -buffer D-1	601	3.92E-04	2.07	10.30	1.200
PbCO ₃ -buffer D-2	601	3.84E-04	2.07	10.32	1.200
PbCO ₃ -buffer E-1	601	8.13E-04	3.2	10.66	1.800
PbCO ₃ -buffer E-2	601	7.86E-04	3.2	10.67	1.800
PbCO ₃ -buffer F-1	601	8.33E-04	3.58	10.79	2.000
PbCO ₃ -buffer F-2	601	8.90E-04	3.58	10.78	2.000
PbCO ₃ -buffer A-1	679	2.15E-05	0.154	9.81	0.100
PbCO ₃ -buffer A-2	679	2.05E-05	0.154	9.80	0.100
PbCO ₃ -buffer B-1	679	5.18E-05	0.49	9.88	0.300
PbCO ₃ -buffer B-2	679	5.06E-05	0.49	9.80	0.300
PbCO ₃ -buffer C-1	679	1.93E-04	1.34	10.04	0.800
PbCO ₃ -buffer C-2	679	1.90E-04	1.34	10.04	0.800
PbCO ₃ -buffer D-1	679	3.75E-04	2.07	10.27	1.200
PbCO ₃ -buffer D-2	679	3.99E-04	2.07	10.28	1.200
PbCO ₃ -buffer E-1	679	7.89E-04	3.2	10.62	1.800
PbCO ₃ -buffer E-2	679	7.95E-04	3.2	10.62	1.800
PbCO ₃ -buffer F-1	679	9.29E-04	3.58	10.73	2.000
PbCO ₃ -buffer F-2	679	9.35E-04	3.58	10.73	2.000
PbCO ₃ -buffer A-1	720	1.98E-05	0.154	9.81	0.100
PbCO ₃ -buffer A-2	720	1.96E-05	0.154	9.80	0.100
PbCO ₃ -buffer B-1	720	5.03E-05	0.49	9.80	0.300
PbCO ₃ -buffer B-2	720	5.01E-05	0.49	9.80	0.300
PbCO ₃ -buffer C-1	720	1.81E-04	1.34	10.04	0.800
PbCO ₃ -buffer C-2	720	1.89E-04	1.34	10.04	0.800
PbCO ₃ -buffer D-1	720	3.55E-04	2.07	10.26	1.200
PbCO ₃ -buffer D-2	720	3.66E-04	2.07	10.27	1.200
PbCO ₃ -buffer E-1	720	7.55E-04	3.2	10.62	1.800
PbCO ₃ -buffer E-2	720	7.64E-04	3.2	10.62	1.800

^a pH readings obtained using a pH electrode were first converted to hydrogen ion concentrations on molar scale (pH) by applying correction factors compiled [16], and then converted to hydrogen ion concentrations on molal scale (pmH) using the equation of Xiong et al. [17]

Fig. 1 Total dissolved lead concentrations [$\Sigma\text{Pb(II)}/\text{mol kg}^{-1}$] in contact with cerussite in $\text{NaHCO}_3 + \text{NaCl}$ solutions as a function of experimental time

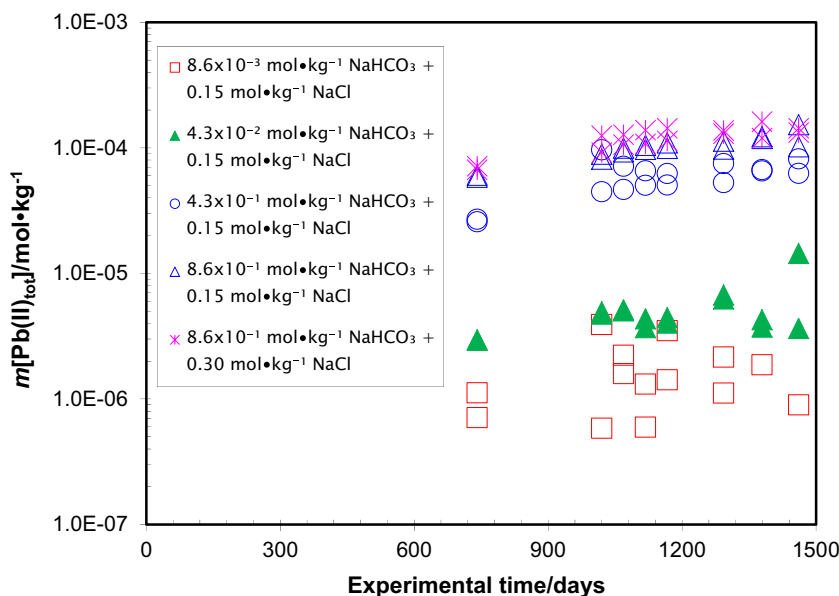
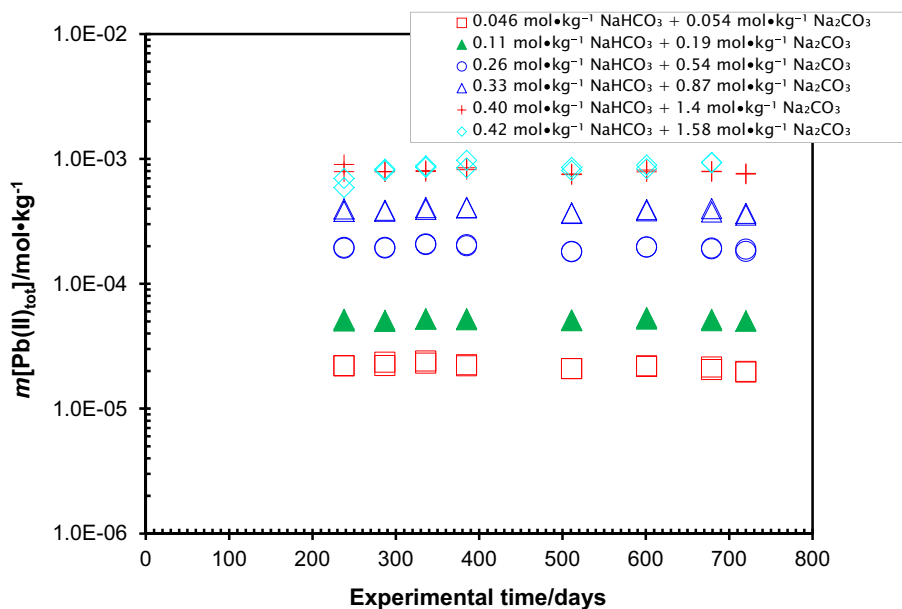
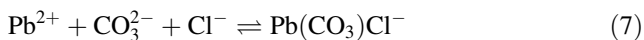


Fig. 2 Total dissolved lead concentrations [$\Sigma\text{Pb(II)}/\text{mol kg}^{-1}$] in contact with cerussite in $\text{NaHCO}_3 + \text{Na}_2\text{CO}_3$ solutions as a function of experimental time



$$\beta_2^0 = \frac{a_{\text{Pb}(\text{CO}_3)_2^{2-}}}{a_{\text{Pb}^{2+}} \times (a_{\text{CO}_3^{2-}})^2} \quad (6)$$

The cumulative formation reaction for the $\text{Pb}(\text{CO}_3)\text{Cl}^-$ complex is as follows:



The corresponding cumulative formation constant for this ternary complex at infinite dilution is as follows:

$$\beta_{11}^0 = \frac{a_{\text{Pb}(\text{CO}_3)\text{Cl}^-}}{a_{\text{Pb}^{2+}} \times a_{\text{CO}_3^{2-}} \times a_{\text{Cl}^-}} \quad (8)$$

In this work, the above cumulative formation constants are taken from the literature [9, 11], and associated Pitzer parameters for the interactions of $\text{PbCO}_3(\text{aq})$ with Cl^- and Na^+ are from Woosley and Millero [9] (Table 3).

Using experimental solubility data of cerussite listed in Tables 1 and 2, $\log K_s^o$ for reaction (1), and the Pitzer parameters associated with $\text{Pb}(\text{CO}_3)\text{Cl}^-$ and $\text{Pb}(\text{CO}_3)_2^{2-}$ are modeled using EQ3/6 Version 8.0a as a modeling platform [12, 13]. The objective function in the modeling is to minimize the difference between experimental and model predicted values. The detailed descriptions about the modeling can be found in previous, similar publications, e.g., [2].

Fig. 3 Plot showing dissolved total lead concentrations in equilibrium with cerussite as a function of total ionic strength in $\text{NaHCO}_3 + \text{NaCl}$ solutions in comparison with the model-predicted values

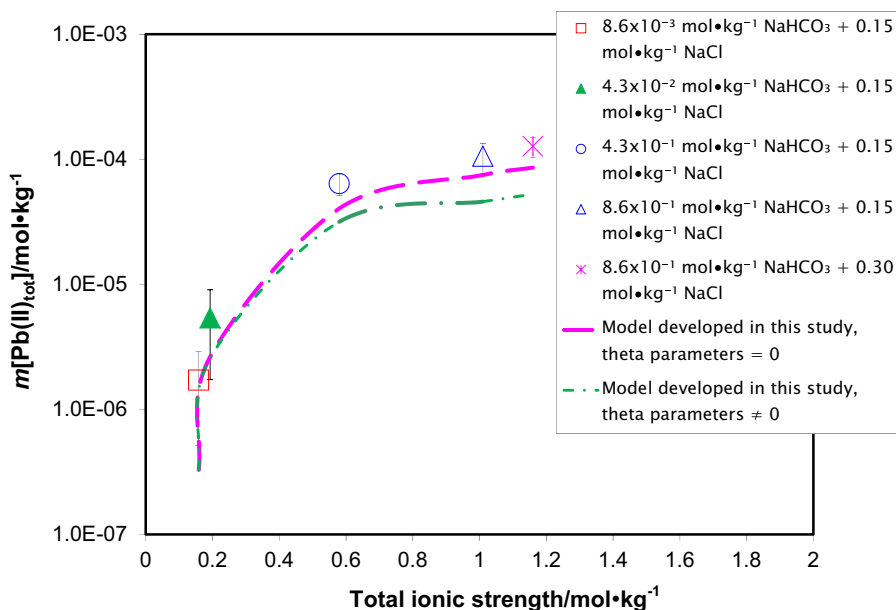
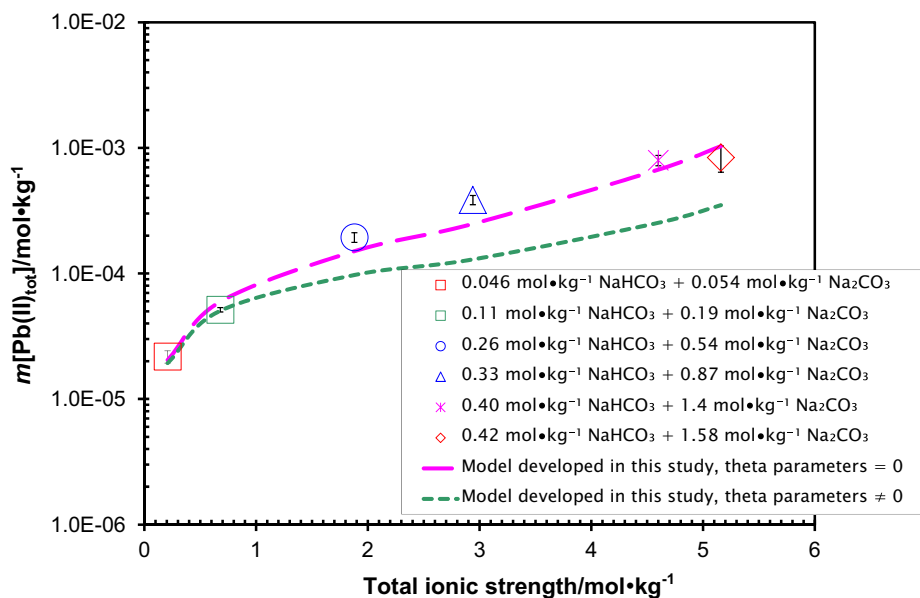


Fig. 4 Plot showing dissolved total lead concentrations in equilibrium with cerussite as a function of total ionic strength in $\text{NaHCO}_3 + \text{Na}_2\text{CO}_3$ solutions in comparison with the model-predicted values



Tabulated in Tables 3 and 4 are the $\log K_s^0$, and Pitzer parameter associated with $\log \beta_1^0$, $\log \beta_2^0$, $\log \beta_{11}^0$ in the $\text{Na}^+ - \text{Pb}^{2+} - \text{Cl}^- - \text{HCO}_3^- - \text{CO}_3^{2-}$ system derived in this study. In Model I, the theta parameters for interactions between HCO_3^- and $\text{Pb}(\text{CO}_3)_2^{2-}$, and between CO_3^{2-} and $\text{Pb}(\text{CO}_3)_2^{2-}$ have non-zero values. In Model II, the theta parameters for interactions between HCO_3^- and $\text{Pb}(\text{CO}_3)_2^{2-}$, and between CO_3^{2-} and $\text{Pb}(\text{CO}_3)_2^{2-}$ have zero values. The model-predicted solubilities of cerussite in the mixtures of $\text{NaCl} + \text{NaHCO}_3$ are compared with the experimental values in Fig. 3. In a set of verification tests, the parameters obtained in this work perform well in

reproducing the experimental solubility data in the mixtures of $\text{NaCl} + \text{NaHCO}_3$, as demonstrated by Fig. 3. Similarly, shown in Fig. 4 are the comparisons of the model-predicted solubilities of cerussite in the mixtures of $\text{NaHCO}_3 + \text{Na}_2\text{CO}_3$ with the experimental values. Again, as illustrated by Fig. 4, the model works well over a wide range of ionic strengths in reproducing the experimental values.

The $\log K_s^0$ [-13.76 ± 0.15 (2σ), and the uncertainty referring to 2σ hereafter in the text] determined in this study is slightly lower than the value of -13.13 at infinite dilution determined by Nasanen et al. [6]. Bilinski and Schindler [7]

Table 3 Equilibrium constants at infinite dilution at 25 °C and 1 bar for the Na⁺-Pb²⁺-Cl⁻-HCO₃⁻-CO₃²⁻ system

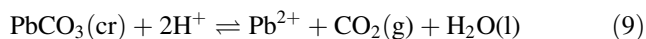
Reactions	log K_s^o , log β_1^o , log β_2^o , or log β_{11}^o	References and remarks
$\text{PbCO}_3(\text{cr}) = \text{Pb}^{2+} + \text{CO}_3^{2-}$	$-13.76 \pm 0.15 (2\sigma)^a$	This study, based on solubility of $\text{PbCO}_3(\text{cr})$ in the mixtures of NaHCO_3 and NaCl and in the mixtures of NaHCO_3 and Na_2CO_3
$\text{Pb}^{2+} + \text{CO}_3^{2-} = \text{PbCO}_3(\text{aq})$	$6.87 \pm 0.09 (2\sigma)$	[9]
$\text{Pb}^{2+} + 2\text{CO}_3^{2-} = \text{Pb}(\text{CO}_3)_2^{2-}$	$10.41 \pm 0.18 (2\sigma)$	[11]
$\text{Pb}^{2+} + \text{CO}_3^{2-} + \text{Cl}^- = \text{Pb}(\text{CO}_3)\text{Cl}^-$	$7.23 \pm 0.74 (2\sigma)$	[9]

^a The errors include the possible error from the small deviation of the experimental temperature from 25 °C

Table 4 Pitzer interaction parameters at 25 °C and 1 bar for the Na⁺-Pb²⁺-Cl⁻-HCO₃⁻-CO₃²⁻ system

Pitzer binary interaction parameters					
Species i	Species j	$\beta^{(0)}$	$\beta^{(1)}$	C^Φ	References
Na ⁺	$\text{Pb}(\text{CO}_3)_2^{2-}$	0.4168	1.74	-0.3161	This study
Na ⁺	$\text{Pb}(\text{CO}_3)\text{Cl}^-$	0.2419	0.29	-0.1802	This study
Pitzer mixing interaction parameters and interaction parameters involving neutral species					
Species i	Species j	Species k	λ_{ij} or θ_{ij}	ζ_{ijk}	References
HCO ₃ ⁻	$\text{Pb}(\text{CO}_3)_2^{2-}$		0.2956		This study, Model I
CO ₃ ²⁻	$\text{Pb}(\text{CO}_3)_2^{2-}$		0.2707		This study, Model I
HCO ₃ ⁻	$\text{Pb}(\text{CO}_3)_2^{2-}$		0		This study, Model II
CO ₃ ²⁻	$\text{Pb}(\text{CO}_3)_2^{2-}$		0		This study, Model II
Cl ⁻	$\text{PbCO}_3(\text{aq})$		-0.02		[9]
Na ⁺	$\text{PbCO}_3(\text{aq})$	Cl ⁻	0	-0.145	[9]

determined the equilibrium quotient (log Q) at 0.3 mol dm⁻³ (0.305 mol kg⁻¹) for the following reaction:



as 5.20 ± 0.03 at 25 °C. Based on the respective Brønsted-Guggenheim-Scatchard specific interaction theory (SIT) coefficients for reaction (9) compiled in [14] and error propagation estimates, the equilibrium constant for reaction (9) at infinite dilution is 4.85 ± 0.10 at 25 °C using the SIT model for extrapolation. According to $\log K = 4.85 \pm 0.10$ at 25 °C and the auxiliary thermodynamic data from [14] for the relevant species in reaction (9), $\Delta_f G_{\text{cerussite}}^0$ is derived as -628.05 ± 0.85 kJ mol⁻¹. Using $\Delta_f G_{\text{cerussite}}^0 = -628.05 \pm 0.85$ kJ mol⁻¹, and $\Delta_f G^0$ for Pb²⁺ and CO₃²⁻ from [14], $\log K_s^o$ for reaction (1) is calculated to be -13.30 ± 0.17 . In comparison, the $\log K_s^o$ determined by this study is -13.76 ± 0.15 , and $\Delta_f G_{\text{cerussite}}^0$ derived from this solubility product constant and the auxiliary thermodynamic data from [14] is -630.68 ± 1.00 kJ mol⁻¹. Considering the fact that the equilibrium quotient for reaction (9) was determined by Bilinski and Schindler [7] in acidic solutions, whereas the

measurements in this study were performed in alkaline solutions, the agreement seems reasonable. The value provided by this study is considered more reliable than the previous values because it is obtained from the long-term solubility data up to 1461 days over a wide range of ionic strengths. In addition, as detailed in the following, the model developed in this study based on these long-term solubility data can reproduce the model-independent solubility data from Bilinski and Schindler [7] with reasonable accuracy. Therefore, in light of those long-term experiments, experimental solubility data produced at Sandia National Laboratories Carlsbad Facility and the thermodynamic parameters obtained based on these data would provide accurate descriptions about the interaction of lead with carbonate in a wide range of ionic strengths.

Bilinski and Schindler [7] performed solubility experiments on cerussite in both mildly alkaline and acidic solutions at 25 °C. In their experiments in the mildly alkaline solutions, they used the mixtures of NaHCO₃ + Na₂CO₃ + NaClO₄ with the total ionic strengths up to 0.4 mol kg⁻¹. In their experiments in acidic solutions, they used the mixtures of HClO₄ and NaClO₄ at various partial

pressures of $\text{CO}_2(\text{g})$. As their experimental data are not used in model development here, they can be used for a validation test of the model. In the validation tests, their concentrations on molar scale are converted to molal scale based on the densities from Söhnel and Novotný [15]. In Fig. 5, the model-predicted solubilities of cerussite from near neutral pmH to mildly alkaline pmH are compared with the experimental values. The model-predicted values compare favorably with the corresponding model-independent experimental values. Notice that the values predicted by the model with zero theta parameters are identical to those predicted by the model with non-zero theta parameters except

for those data points with relatively high concentrations of carbonate such as the data point with $\text{NaHCO}_3 = 0.3 \text{ mol kg}^{-1}$. Similarly, the model-predicted solubilities of cerussite in acidic pmH at various partial pressures of $\text{CO}_2(\text{g})$ ranging from 0.0466 to 0.912 atm are compared with the respective experimental values in Fig. 6. Again, the agreement is excellent. The solubilities predicted by the model with zero theta parameters are identical to those by the model with non-zero theta parameters for all of the data points. This suggests that the theta parameters do not have much effect in the acidic pH range, as carbonic acid is predominantly speciated as $\text{H}_2\text{CO}_3(\text{aq})$ in this pH range.

Fig. 5 Plot showing model-independent solubilities of cerussite represented by dissolved total lead concentrations as a function of hydrogen ion concentrations (pmH) in $\text{NaHCO}_3 + \text{Na}_2\text{CO}_3 + \text{NaClO}_4$ solutions from Bilinski and Schindler [7] in comparison with the model-predicted values

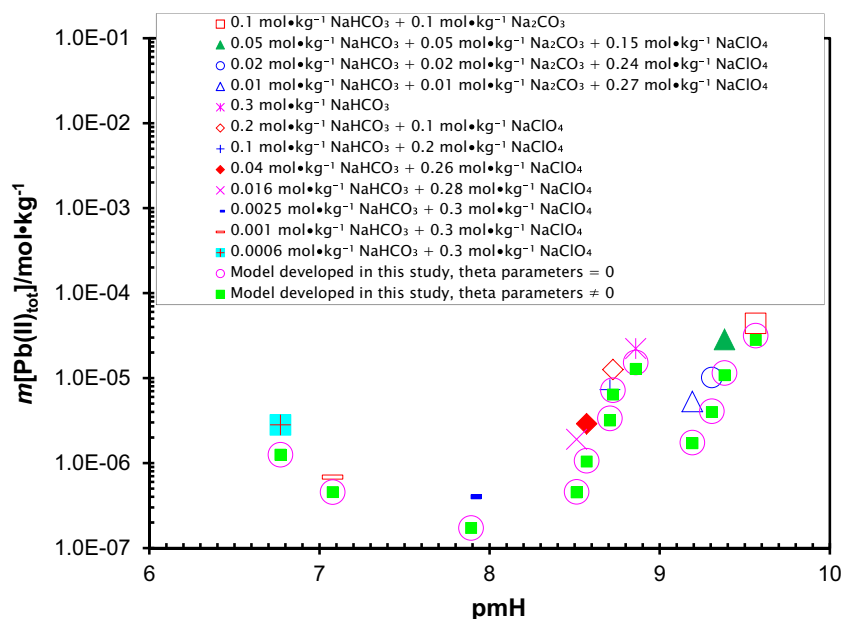
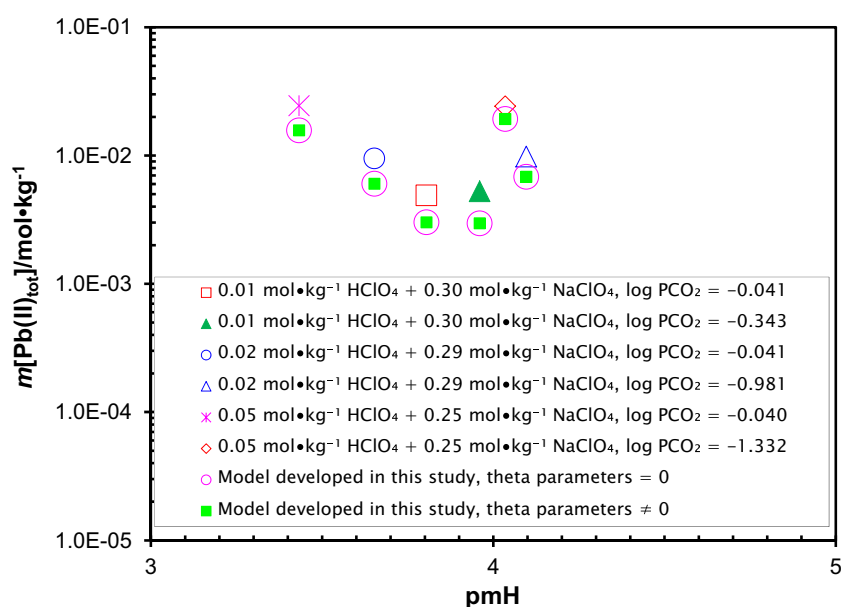


Fig. 6 Plot showing model-independent solubilities of cerussite represented by dissolved total lead concentrations as a function of hydrogen ion concentrations (pmH) in $\text{HClO}_4 + \text{NaClO}_4$ solutions at constant partial pressures of $\text{CO}_2(\text{g})$ from Bilinski and Schindler [7] in comparison with the model-predicted values



Conclusions

Long-term solubility measurements up to 1461 days and to high ionic strengths for cerussite in the mixtures of NaCl and NaHCO₃ and of NaHCO₃ and Na₂CO₃ produced at Sandia National Laboratories Carlsbad Facility are presented in this work. A Pitzer model is developed based on these solubility measurements. This model would provide accurate descriptions about the interaction of lead with carbonate under various conditions with applications to many fields such as nuclear waste management and supergene Pb–Zn ore deposits.

Experimental

In our solubility experiments, about 2 grams of the solubility-controlling material, crystalline lead carbonate, from Alfa Aesar, were weighed out and placed into 150 cm³ plastic bottles. For each experiment, 100 cm³ of various supporting solutions were added to the bottles. Once filled, the lids of the bottles were sealed with parafilm. The supporting electrolytes are a series of NaHCO₃ + NaCl solutions ranging from 0.159 to 1.16 mol kg⁻¹ in total ionic strength, and mixtures of NaHCO₃ + Na₂CO₃ with total ionic strengths ranging from 0.208 to 5.16 mol kg⁻¹. At each ionic strength, replicate experimental runs were set up. The supporting solutions were prepared from the reagent grade chemicals from Fisher Scientific and deionized (DI) water with Ω better than 18.0. Undersaturation experiments were conducted at the laboratory room temperature (295.65 ± 0.5 K).

The pH readings were measured with an Orion-Ross combination pH glass electrode, coupled with an Orion Research EA 940 pH meter that was calibrated with three pH buffers (pH 4, pH 7, and pH 10). In solutions with an ionic strength higher than 0.10 mol kg⁻¹, hydrogen-ion concentrations on molar scale (pCH) were determined from pH readings using correction factors compiled [16]. Based on the equation in Xiong et al. [17], pCHs are converted to hydrogen-ion concentrations on molal scale (pmH).

Solution samples were periodically withdrawn from experimental runs. Before solution samples were taken, pH readings of experimental runs were first measured. The sample size was usually 3 cm³. After a solution sample was withdrawn from an experiment and filtered with a 0.2 μm syringe filter, the filtered solution was then weighed, acidified with 0.5 cm³ of concentrated TraceMetal[®] grade HNO₃ from Fisher Scientific, and finally diluted to a volume of 10 cm³ with DI water. If subsequent dilutions were needed, aliquots were taken from the first dilution samples for the second dilution, and aliquots of the second dilution were then taken for further dilutions.

Lead concentrations of solutions were analyzed with a Perkin Elmer dual-view inductively coupled plasma-atomic emission spectrometer (ICP-AES) (Perkin Elmer DV 3300). Calibration blanks and standards were precisely matched with experimental matrices. The linear correlation coefficients of calibration curves in all measurements were better than 0.9995. The analytical precision for ICP-AES is better than 1.00 % in terms of the relative standard deviation (RSD) based on replicate analyses.

Solid phase was analyzed using a Bruker D8 Advance X-ray diffractometer with a Sol-X detector. There was no phase change during the experiments.

Acknowledgments This research is funded by WIPP programs administered by the Office of Environmental Management (EM) of the U.S Department of Energy. The author is grateful to Leslie Kirkes and Terry Westfall for their major efforts in the data acquisition. The laboratory assistance from Diana Goulding, Brittany Hoard, Cassandra Marrs, Rachael Roselle, Tana Saul, and Kira Vicent is gratefully acknowledged. The author wishes to express his gratitude to two journal reviewers for their insightful and thorough reviews, and to Dr. Heinz Gamsjäger, the Associate Editor, for his editorial efforts.

References

1. Gamsjäger H, Fluch A, Swinehart JH (1984) *Monatsh Chem* 115:251
2. Xiong Y-L, Kirkes L, Westfall T, Roselle R (2013) *Chem Geol* 342:128
3. Pirajno F, Burlow R, Huston D (2010) *Ore Geol Rev* 37:101
4. Xiong Y-L, Lord ACS (2008) *Appl Geochem* 23:1634
5. Taylor P, Lopata VT (1984) *Can J Chem* 62:395
6. Nasanen R, Merilainen P, Leppanen K (1961) *Acta Chem Scand* 15:913
7. Bilinski H, Schindler P (1982) *Geochim Cosmochim Acta* 46:921
8. Powell KJ, Brown PL, Byrne RH, Gajda T, Hefter G, Luez A-K, Sjöberg S, Wanner H (2009) *Pure Appl Chem* 81:2425
9. Woosley RJ, Millero FJ (2013) *Marine Chem* 149:1
10. Millero FJ, Byrne RH (1984) *Geochim Cosmochim Acta* 48:1145
11. Easley RA, Byrne RH (2011) *Geochim Cosmochim Acta* 75:5638
12. Wolery TJ, Xiong Y-L, Long J (2010) *Verification and Validation Plan/Validation Document for EQ3/6 Version 8.0a for Actinide Chemistry*, Document Version 8.10. ERMS 550239. Sandia National Laboratories, Carlsbad, NM
13. Xiong Y-L (2011) *WIPP Verification and Validation Plan/Validation Document for EQ3/6 Version 8.0a for Actinide Chemistry*, Revision 1, Document Version 8.20. ERMS 555358, supersedes ERMS 550239. Sandia National Laboratories, Carlsbad, NM
14. Gamsjäger H, Gajda T, Sangster J, Saxena SK, Voigt W (2012) *Chemical Thermodynamics of Tin*. Chemical Thermodynamics, vol 12. Elsevier, Amsterdam
15. Söhnel O, Novotný P (1985) *Densities of aqueous solutions of inorganic substances*. Elsevier, New York
16. Roselle G (2012) SP12-14 Use of pH meter and electrode, Revision 3. Sandia National Laboratories, Carlsbad, NM
17. Xiong Y-L, Deng H-R, Nemer M, Johnsen S (2010) *Geochim Cosmochim Acta* 74:4605